

Visual-Language-Guided Task Planning for Horticultural Robots

Jose Cuaran^{1*}, Kendall Koe^{1*}, Aditya Potnis¹, Naveen Kumar Uppalapati³, and Girish Chowdhary^{1,2}

Abstract—Crop monitoring is essential for precision agriculture, but current systems lack high-level reasoning. We introduce a novel, modular framework that uses a Visual Language Model (VLM) to guide robotic task planning, interleaving input queries with action primitives. We contribute a comprehensive benchmark for short- and long-horizon crop monitoring tasks in monoculture and polyculture environments. Our main results show that VLMs perform robustly for short-horizon tasks (comparable to human success), but exhibit significant performance degradation in challenging long-horizon tasks. Critically, the system fails when relying on noisy semantic maps, demonstrating a key limitation in current VLM context grounding for sustained robotic operations. This work offers a deployable framework and critical insights into VLM capabilities and shortcomings for complex agricultural robotics.

<https://kendallkoe.com/Visual-Language-Guided-Task-Planning-for-Horticultural-Robots/>.

Index Terms—Task Planning, Foundation Models, Vision-Language Models, Agricultural Robotics

I. INTRODUCTION

The agricultural sector is under increasing pressure to meet the global demand for food while facing persistent labor shortages, climate variability, and sustainability challenges. Precision agriculture has emerged as a response, leveraging data-driven technologies to optimize resource use, improve productivity, and minimize environmental impact. Central to this approach is crop monitoring, which enables continuous assessment of plant health, early detection of pests and nutrient deficiencies, and precise management of irrigation and fertilization [1]. In recent years, robotics has become an essential component of precision agriculture, automating key tasks such as soil preparation, planting, weeding, harvesting, and phenotyping across diverse environments including fields, orchards, and greenhouses [2]. These advances pave the way for intelligent horticultural robots capable of not only perceiving and acting within complex crop environments but also reasoning about high-level monitoring tasks.

In horticultural environments, mobile manipulator robots show strong potential for active data collection and crop monitoring. Prior work has demonstrated their effectiveness for target-aware mapping and viewpoint planning [3]–[7]. However, most existing approaches focus on a single target type (e.g., leaves, fruits, or stems) within a single crop,

and rely on a fixed mapping or sensing strategy. In real farming scenarios, monitoring needs are substantially more diverse. Growers may wish to perform different types of scans—such as dense 3D reconstruction of fruit clusters, sparse sampling for disease inspection, or targeted imaging of stems—across multiple plant parts and crop types within the same environment. Supporting this flexibility is critical, as such data underpins a wide range of downstream agricultural tasks, including precision pesticide application, harvest readiness assessment, and pruning or canopy management. Ideally, these capabilities should be accessible through intuitive human–robot interaction. Rather than configuring low-level sensing or planning objectives, a farmer should be able to specify high-level goals in natural language (e.g., “go to the tomato plants and collect 50 images of ripe fruits”), which the robot can interpret, decompose into subtasks, and execute autonomously. This paradigm shifts mobile manipulation from narrowly specialized sensing systems toward general-purpose agricultural assistants capable of adapting to evolving monitoring needs.

The rise of Large Language Models (LLMs) and Vision-Language Models (VLMs) has marked a paradigm shift for task planning in robotics, enabling zero-shot task decomposition from natural language instructions into low-level plans for navigation and manipulation in different domains [8]–[11]. VLMs extend this capability by directly interpreting visual inputs, supporting applications such as action scoring, object relationship extraction, success detection, and traversability assessment [12]–[17], often augmented by maps for spatial context [18]–[22]. Object-goal navigation and instruction following have been the main focus of these works.

Despite these advancements, the integration of LLMs and VLMs into agricultural robotics lags behind other domains. Applications in agriculture have primarily focused on disease and pest detection [23], with limited exploration of task planning. Notable exceptions include AgriVNL, which employs VLMs for long-horizon navigation tasks in agricultural scenarios leveraging camera observations only. A concurrent work uses an LLM to generate behavior trees for mission planning using textual farm layout descriptions [24]. However, these methods suffer from poor spatial reasoning as they rely on camera images or text descriptions only.

To address these gaps, we propose a VLM-driven framework for task planning in agricultural mobile manipulator robots, aimed at user-friendly crop monitoring in horticultural

*Equal Contribution. The authors are with (1) the Siebel School of Computing and Data Science, (2) the Department of Agricultural and Biological Engineering and (3) National Center for Supercomputing Applications at University of Illinois, Urbana-Champaign.

Correspondence to {jrc9,girishc}@illinois.edu

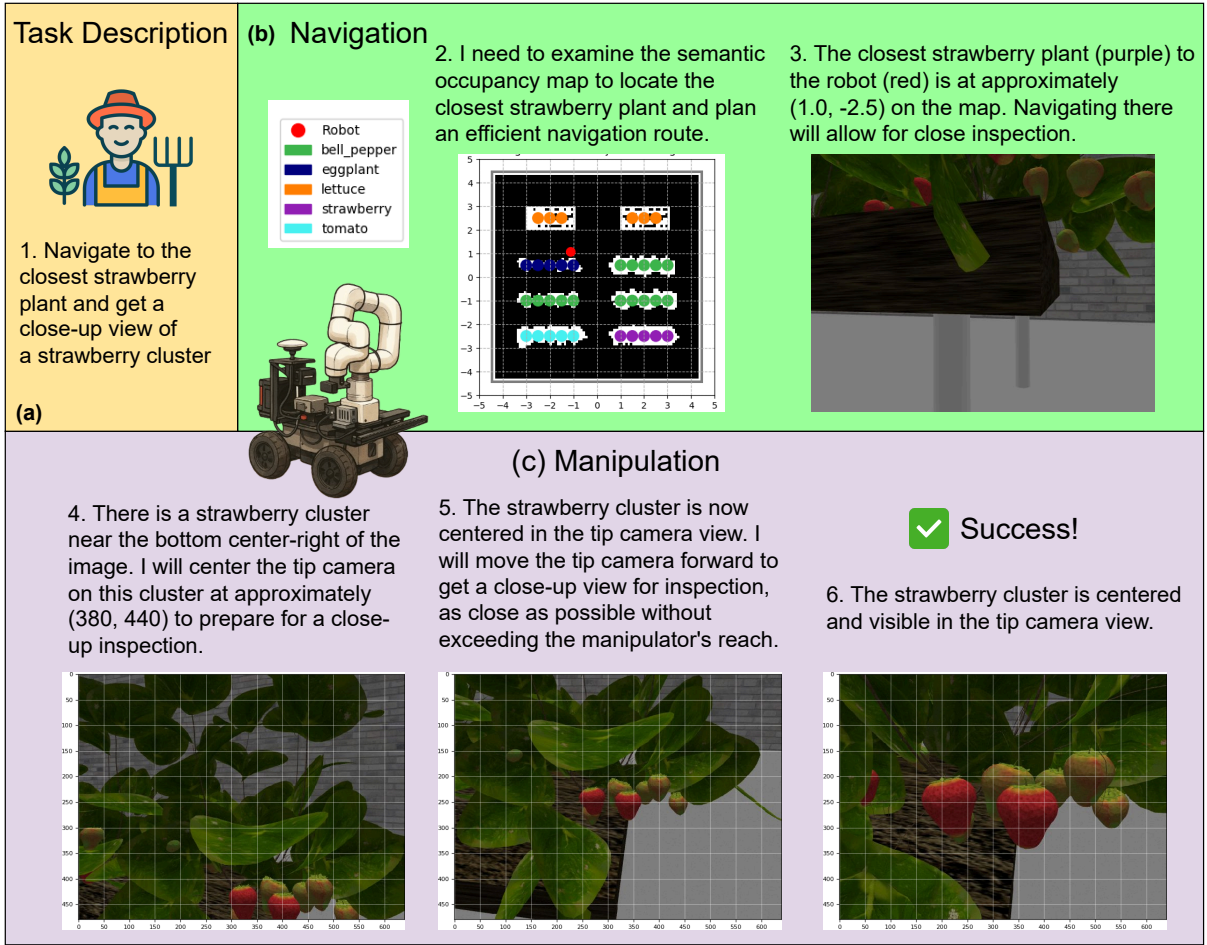


Fig. 1. Sample episode of a single-plant, single-target monitoring task executed by the VLM agent. (a) The VLM takes as input the task prompt, the context and tools description. (b) The navigation tool call is used to navigate to the goal object and (c) The manipulation tools are invoked at different time steps until completing the inspection task.

settings such as greenhouses. Building on prior work that employs LLMs and VLMs for task planning, our approach integrates multiple sources of information—such as camera observations and top-down maps—processed in different ways to support decision making. Rather than supplying all this data to the VLM at every step, we encourage the model to query input sources selectively and efficiently. This design allows the robot to combine heterogeneous information with available navigation and manipulation primitives to complete instructions successfully. Our framework supports targeted exploration and data collection driven by natural language commands, offering both flexibility and efficiency. To the best of our knowledge, this is the first work to introduce visual-language-guided crop monitoring in agricultural environments.

In summary, the main contributions of this paper are:

- A novel, modular framework for task planning in horticultural environments that interleaves input-source queries with action-primitive callbacks.

- A benchmark for both short and long horizon tasks for crop monitoring in horticultural scenarios, including a lightweight simulation environment.

II. RELATED WORKS

Task planning for robotics has been extensively studied long before the rise of large language and vision-language models. Classical approaches relied on symbolic reasoning systems such as STRIPS [25] and Hierarchical Task Networks (HTNs) [26], [27]. While these methods provide strong guarantees in structured settings, they are limited by the need for accurate, handcrafted domain models, making them unfeasible in unstructured or partially observable environments such as agricultural settings. Learning-based methods, including reinforcement learning and imitation learning, have also been explored to couple perception and planning [28]. However, they typically require large amounts of task-specific training data and generalize poorly to novel instructions or unseen environments.

More recently, large foundation models have shown impressive capabilities for navigation and manipulation task planning in a zero-shot manner, that is, without any fine-tuning. Their general knowledge enables them to extract relationships between objects, places, and actions, which is fundamental for planning and decision making. They have also enabled instruction following from natural language commands. We focus this review on such models, and more specifically on the use of LLMs and VLMs for task planning in mobile-manipulation agents.

LLMs and VLMs in General Domains

LLMs have demonstrated task planning capabilities since the early days of these models. For instance, [8] showed that LLMs can decompose language instructions into mid-level plans for mobile-manipulation tasks in indoor environments, using only a few demonstration examples of related tasks and without additional training. Several approaches have emerged to improve the performance of these models, including the use of pre-trained value functions to weight the skills proposed by LLMs for better grounding in the real world [9]. LLMs can also take feedback from different sources (e.g., scene description models, object detectors, or humans in the loop) to improve problem-solving tasks for embodied agents [10]. Additionally, the coding capabilities of these models have been leveraged to generate language model programs (LMPs) that manage action primitives to solve complex and long-horizon tasks [11].

With the advent of VLMs, models no longer require explicit scene descriptions as input, since they can directly process images, overcoming a key limitation of LLMs. Simple approaches take images as input with potential actions superimposed on them (e.g., polar actions in [12]). The models then either assign scores to these actions or directly choose one for execution [12], [13], simplifying the classical perception–planning–control pipeline. VLMs have also been leveraged to extract various forms of information from camera observations, including object descriptions [14], success/failure detection [15], action-conditioned relationships between objects (e.g., opening a drawer reveals a toy) [16], and traversability estimation [17].

More complex methods incorporate maps to support decision making. Different types of maps have been proposed. Visual language maps, typically dense representations with visual–language features (e.g., CLIP embeddings), enable object position retrieval, where an LLM can parse the instructions into object queries [18]. Similarly, topological maps and 3D scene graphs can store semantic features in their nodes more efficiently, making them suitable for larger environments [19], [20]. While these maps allow objects to be retrieved in natural language, they provide limited spatial context to the LLM.

To address the lack of spatial awareness in previous works, [21] proposed MapGPT, where a topological map encoded in linguistic form is provided to the LLM. This enables the agent to understand spatial structures to some degree, but

still omits essential metric information such as object shapes, sizes, and explored/unexplored regions. A closer approach to ours is [22], which uses a top-down map containing key areas, objects labels, historical traversed regions, and frontier segments as input to a VLM. The model assigns scores to key areas related to the location of a target object. In contrast, we show that combining global maps, egocentric maps, and camera observations allows a VLM to directly execute action primitives for exploration and monitoring tasks.

LLMs and VLMs for Question Answering

One of the earliest efforts to connect language models with robotic planning is SayCan [9], which combines LLM-generated high-level instructions with affordance value functions representing the feasibility of pre-trained robotic skills. By grounding semantic reasoning in physical affordances, SayCan enabled mobile manipulators to perform over a hundred real-world kitchen tasks with impressive planning accuracy. Building on this insight, the CAPE [29] framework introduced corrective planning mechanisms, allowing an LLM to suggest recovery actions when preconditions were violated. CAPE significantly improved robustness across both simulated and real-world environments, demonstrating how retrieval and feedback loops can address weaknesses in static LLM-driven plans.

Parallel work has explored structuring robot policies to increase interpretability and resilience. For instance, BETR-XP-LLM [30] dynamically expands behavior trees through LLM-guided reasoning, enabling robots to generate transparent and verifiable plans that adapt to execution challenges. By representing actions as structured tree nodes, this line of work connects the flexibility of language models with the reliability of symbolic planning, offering a more trustworthy substrate for embodied decision-making.

Recent studies have extended these ideas to embodied question answering (EQA) and long-horizon reasoning. OpenEQA [31] formalized EQA benchmarks to evaluate foundation models in robotic environments, positioning language-guided visual reasoning as a critical capability. Building on this benchmark, [32] introduced memory-augmented reasoning that allows robots to recall and plan across extended temporal horizons. Similarly, [33] proposed self-generated memory as a way to ground VLM predictions in past experience, improving fidelity in sequential tasks. Collectively, these works shift the focus from single-shot responses toward temporally coherent reasoning, which is essential for embodied applications.

Another frontier in this space integrates visual grounding and closed-loop control. [34] provided early evidence that VLMs can generate high-level robotic plans from visual input, establishing the viability of multimodal foundation models for action planning. In [15], the framework proposed extended this approach by embedding feedback mechanisms into VLM-driven manipulation, allowing robots not only to propose actions but also to verify success and adjust dynamically. These studies demonstrate the growing role of

vision-language models in bridging perception and planning through feedback, complementing the affordance-based and memory-based approaches described above.

Yet despite these advances, little work explores how such embodied reasoning can be applied in agricultural contexts, where the need to integrate perception, planning, and execution is equally critical but underexplored.

LLMs and VLMs in Agricultural Environments

The application of LLMs and VLMs in agriculture has primarily focused on disease and pest detection, rather than full robotic autonomy [23]. Several recent works have aimed to adapt foundation models for agricultural domains. For instance, AgriCLIP adapts CLIP via domain-specialized cross-model alignment, improving performance on tasks involving crops and livestock by leveraging agricultural-specific image-text pairs [35]. Similarly, AgroGPT demonstrates an efficient agricultural vision-language model with expert tuning, allowing the model to handle diverse visual inspection tasks with high accuracy [36]. Other studies have explored VLMs for crop disease diagnosis: a visual large language model for wheat disease detection in the wild [37], SCOLD for leaf disease identification [38], and few-shot image classification of crop diseases using vision-language models [39]. These approaches indicate the potential of VLMs to generalize across multiple crops and disease types with limited labeled data.

To systematically evaluate these models, agricultural benchmarks such as AgroBench provide a broad set of 682 disease categories across multiple crops, enabling consistent comparison of model performance in zero-shot and few-shot settings [40]. SCOLD further contributes with 186,000 image-text pairs for fine-grained disease identification [38]. AgriVLM, a separate framework, has also achieved over 90% accuracy in identifying disease and growth stages, demonstrating the promise of vision-language reasoning in practical agricultural applications [41].

While most prior work focuses on classification and recognition, there are early attempts to incorporate these models into robotic pipelines. AgriVLM enables visual-language navigation in agricultural scenes, decomposing language instructions into subtasks and outputting low-level actions to navigate from start to destination [23]. Zuzuarregui et al. (2025) propose mission planning in agricultural environments using an LLM with textual farm layouts, but find spatial reasoning is limited when key spatial features are provided only in text [24]. In contrast, our approach allows a VLM to query multiple sources information actively, improving crop monitoring efficiency while integrating perception, planning, and action in real-time.

III. METHODS

In this work, we aim to perform crop monitoring tasks in horticultural environments using a mobile manipulator controlled by a VLM. Specifically, the robot starts from an arbitrary position in an unknown environment and is given a crop monitoring task defined by one or more plant

targets (e.g., tomato or bell pepper plants) and one or more inspection targets (e.g., a tomato cluster or a stem). The objective is for the VLM to leverage a set of perception and action tools to efficiently accomplish the assigned task.

Figure 2 presents an overview of our system. The robotic platform consists of a mobile manipulator equipped with two RGBD cameras: one fixed to the front of the robot base and another mounted on the manipulator’s end-effector. Our approach focuses on providing the VLM with a diverse set of perception and action tools that enable decision-making for both global and local navigation, as well as precise target inspection using the end-effector camera. A key component of our system is a semantic occupancy map, which encodes information about both scene occupancy and object locations. This map serves two main purposes: it supports the classical navigation stack to ensure safe and efficient path planning, and it provides spatial context for high-level decision-making by the VLM.

A. Perception

Open-Vocabulary Semantic Occupancy Map. Inspired by prior work on semantic mapping that leverages visual-language features (e.g., CLIP) to create open-vocabulary maps [18], we build a semantic map of sparse objects modeled as spheres and semantic feature vectors. Our mapping approach is presented in Fig. 3. We use Detic for open-vocabulary detection and segmentation. This allows us to construct semantic maps with a customizable set of categories without fine-tuning on specific crop types. Each detected object is tracked over time using a Kalman filter, which fuses multiple observations to update its position, size, and confidence. This combination of an efficient detector and compact object representation allows our mapping pipeline to operate in real time, a critical property for robotic applications.

In parallel, we maintain an OctoMap [42] built from RGBD observations, encoding free, occupied, and unknown regions. By projecting both the 3D semantic objects and the occupancy map into a top-down view, we generate a 2D semantic occupancy map that integrates occupancy information, object locations, and semantic confidence. This map is provided to the VLM for decision-making, supporting exploration and object-goal navigation tasks.

Enriched Camera Image Observations. To address the spatial reasoning limitations of current VLMs, we preprocess images from both the base and end-effector cameras. Following prior works [12], we project polar action commands from the robot coordinate frame onto the base camera image plane. This enables the VLM to reason directly in the image space and navigate toward visible target points. For the tip camera, we superimpose a 2D grid onto the image, allowing the VLM to more precisely localize objects in image coordinates. These 2D locations are then projected into 3D coordinates using the corresponding depth image and camera intrinsics. This preprocessing step allows the VLM to plan both navigation and manipulation actions in the image

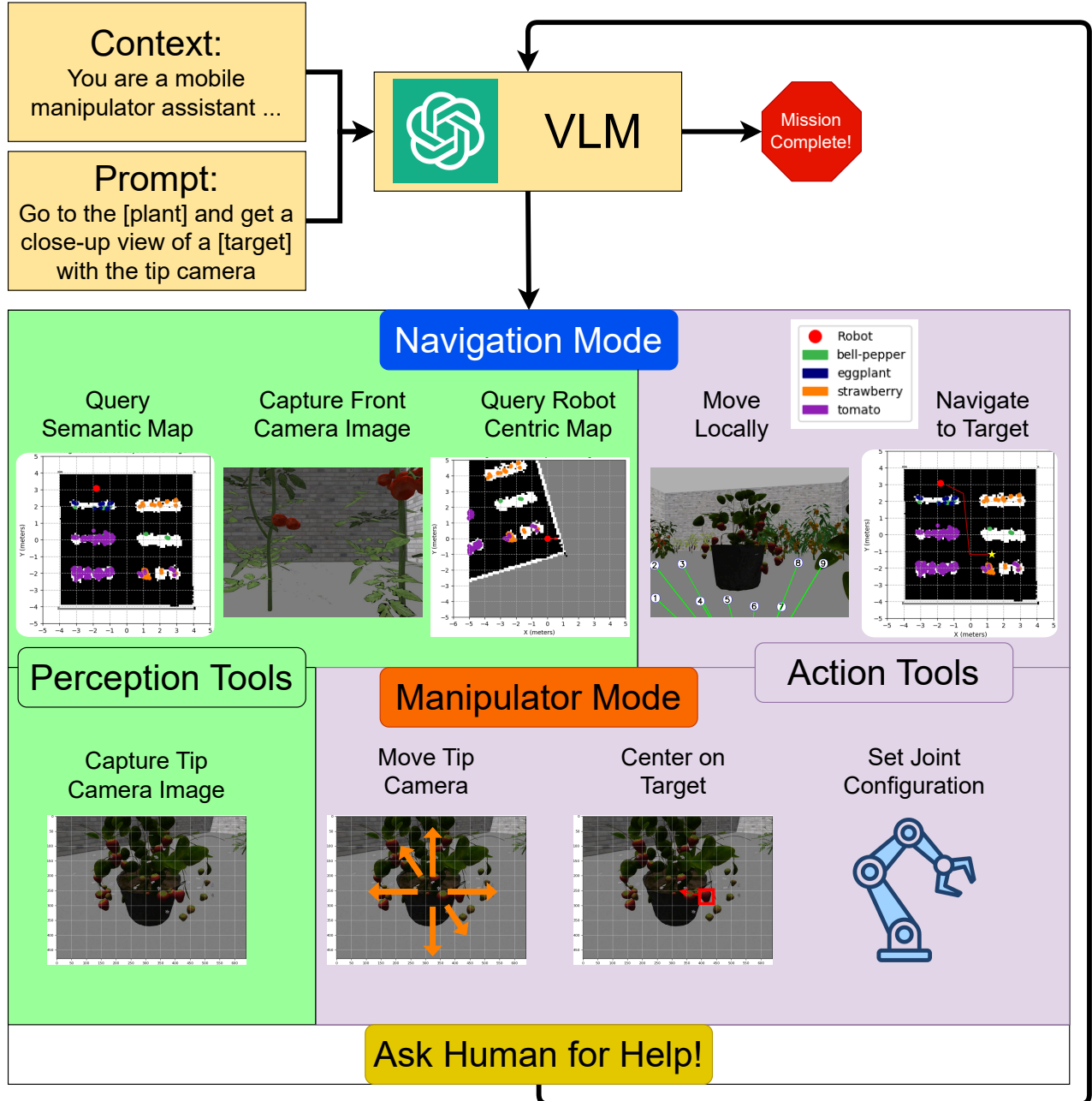


Fig. 2. **Overall System Pipeline** Given context and the assigned task, the agricultural agent selects from a library of action primitives to achieve the task. The agent can switch between manipulation and navigation modes. A library of primitive tasks are available for the agent to choose from to accomplish the task. Once the task is complete or the agent requires help, a human can be prompted to intervene.

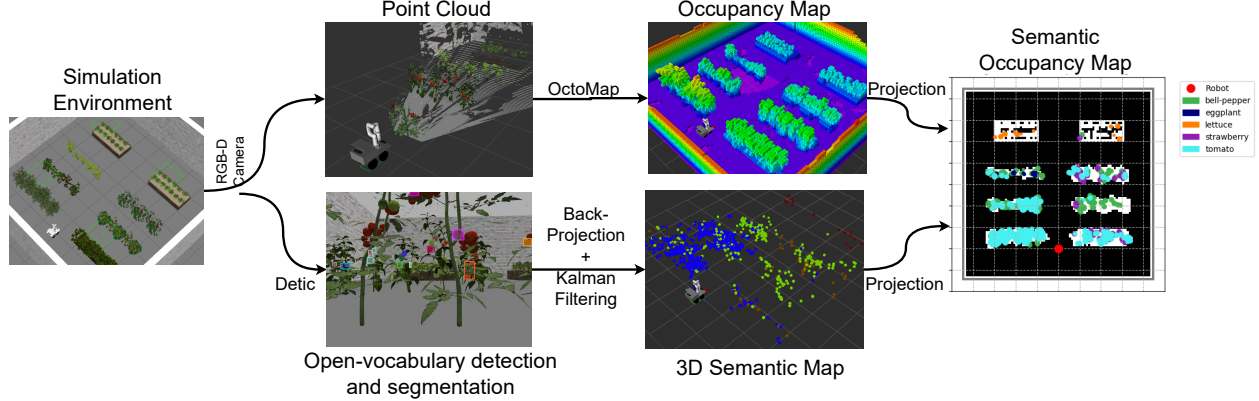


Fig. 3. Semantic mapping pipeline. The RGBD data is used to generate an occupancy map of the environment. Detic is used for open vocabulary object detection and segmentation. The output is backprojected and filtered with kalman filtering. Both branches are projected to create a semantic occupancy map.

domain, which are then executed by the robot's low-level controllers.

B. Planning

Task Planner. We employ a VLM agent to orchestrate a set of perception and action primitives in order to accomplish a task. The model receives three main inputs: a context description, descriptions of available perception and action primitives, and the task instruction in natural language.

Unlike prior approaches that generate a full program of primitive actions (i.e., a language model program, or LMP [11]), our VLM agent operates iteratively: at each time step, it outputs the next tool or task to execute, receives feedback from the execution, and performs online replanning. This design is crucial because horticultural environments are partially observable. For instance, a fruit of interest might be occluded by leaves or out of the current field of view, making predefined action sequences unreliable without feedback. We also maintain a history of tool calls and outcomes, allowing the agent to reason over past experiences. However, for efficiency and relevance, we only include the most recent image observation in the context window.

Context description. This includes information about the robot configuration, available data sources (e.g., map, RGBD images), and a set of behavioral rules promoting safety, motion efficiency, high-quality image capture, failure recovery, and proper stopping conditions.

Tool descriptions. For each perception or action tool, we specify its purpose, input arguments, and expected outputs. We also prompt the VLM to justify each tool selection with a brief reasoning statement to enhance interpretability and traceability of its decisions.

Task specification. Tasks are provided in natural language and typically involve one or more navigation targets (e.g., specific plants) and inspection targets (e.g., fruits, stems or leaves).

Navigation and Manipulation Primitives. We implement a set of tools for global navigation (e.g., navigate-to-map-

point), local navigation (e.g., rotate-and-move-forward), and manipulation (e.g., move-tip-camera-left). The complete list of available tools is provided in the supplementary material.

While the semantic map allows the VLM to identify the approximate location of objects, relying solely on it is insufficient because the map may contain false positives or inaccurate object positions due to perception noise. Therefore, we also provide robot-centric representations, enabling more accurate localization and short-range navigation adjustments (e.g., fine-tuning orientation or moving forward). Alternatively, the base camera image with superimposed polar actions described in the previous section can be used for local motion planning.

For manipulation, we include primitive motions for the tip camera along the six Cartesian directions (left, right, up, down, forward, and backward). We also design a centering tool that automatically aligns an object of interest with the camera's optical center providing a more efficient and flexible alternative to fixed-step movement commands.

C. Control

For low-level motion planning, we employ the ROS MoveBase and MoveIt packages, ensuring collision-free navigation and manipulation. Both components leverage the occupancy map to plan safe trajectories for the mobile base and the manipulator.

IV. EXPERIMENTS

A. Simulation Environment

We evaluated our system in three Gazebo simulation environments modeled after realistic greenhouse layouts. Sample viewpoints from each scene are shown in Fig. 4. In all scenes, crops are arranged in rows spaced 1.5 m apart center-to-center. The first and simplest scene is a tomato monoculture. Tomatoes are a high-value crop commonly grown this way [43], [44]. Tomato plants with varying geometry and fruits at different ripeness stages were randomly placed throughout four rows. The second scene increases complexity

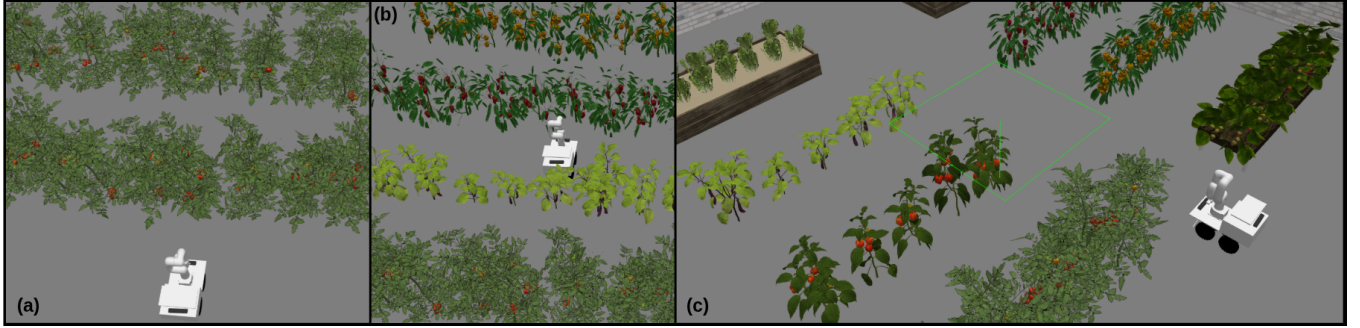


Fig. 4. **Simulation Environments** Three gazebo simulation environments are used to evaluate the system. (a) A monoculture environment filled with various ripe and unripe tomatoes. (b) A polyculture environment filled with tomatoes, orange peppers, red peppers, and eggplants. (c) A polyculture environments filled with tomatoes, green peppers, red peppers, and eggplants as well as lettuce and strawberries on raised tables.

by introducing a polyculture: tomatoes, eggplants, orange bell peppers, and red bell peppers. Each crop type occupies a single row, resulting in four distinct rows and greater visual variety for the VLM. The third and most complex scene includes all crops from the second scene and adds lettuce and strawberries. These additional crops are placed in raised planters, reflecting common agricultural practice and contributing more geometric variation. The six crop varieties each occupy their own row, with an additional row of tomatoes and lettuce. The scene is arranged as two columns of four rows, with a central aisle to improve access to the plants.

B. Metrics

We report the *success rate* and *task completion rate* as indicators of task efficacy. We also report the *number of tool calls* as an indicator of efficiency, and finally, the *success rate weighted by shortest path length* as an indicator of navigation success and efficiency.

To compute the success rate and task completion rate, we divide each task into multiple subgoals, including both navigation and manipulation subgoals. For example, the task “*navigate to three tomato plants and take two pictures from each — one of a green tomato and one of a ripe tomato*” is split into three navigation subgoals and six manipulation subgoals. An episode is considered successful if all of its subgoals are successfully completed. The success rate SR is computed as:

$$SR = \frac{1}{N} \sum_{i=1}^N S_i$$

where $S_i \in \{0, 1\}$ is the success indicator for episode i , and N is the total number of episodes.

The completeness score C_i for episode i is computed as the ratio between the number of successfully completed subgoals and the total number of subgoals in that episode. We then compute the average task completion rate TCR as:

$$TCR = \frac{1}{N} \sum_{i=1}^N C_i$$

We report the number of tool calls as the total number of perception and action primitives invoked to complete a task. This metric is averaged across the successful episodes only, since partially completed tasks can lead to an underestimation of the actual number of required tool calls.

We compute the success rate weighted by shortest path length SPL following [45]:

$$SPL = \frac{1}{N} \sum_{i=1}^N S_i \frac{l_i}{\max(l_i, p_i)}$$

where p_i is the distance traveled by the agent. Unlike [45], where l_i represents the shortest path length, we define l_i as the distance traveled by the human expert. This is due to the fact that finding the true optimal path requires identifying the optimal sequence of plant targets to visit, which is cumbersome in our environments containing multiple crop instances distributed across different rows. Despite this assumption, our SPL remains a reliable indicator of navigation success and efficiency relative to human experts, as it penalizes long or inefficient trajectories while rewarding both successful and efficient navigation behavior.

C. Benchmark Description

Task categories. We split the tasks into four types based on complexity: (1) Single Plant, Single Target, (2) Single Plant, Multiple Targets, (3) Multiple Plants, Single Target, and (4) Multiple Plants, Multiple Targets. Each task prompt requires the robot to navigate to a specified plant and monitor one or more target parts of that plant. We randomize the plant type, the target plant parts (leaves, stems, fruits), the number of plants (one to three), the number of target parts (one to three), characteristics of the target part (e.g., ripe tomato, red bell pepper), and the initial robot pose within the environment. To increase linguistic diversity, we use an LLM to paraphrase the natural-language prompts. We run 20 prompts per environment for tasks involving a single plant, and 10 prompts per environment for tasks involving multiple plants. In total, the evaluation consists of 198 tasks, divided into three groups and executed by three human experts and the VLM agent.

VLM agent. We use GPT-4.1 as the VLM agent via the OpenAI API with tool-calling capabilities. In this study, we evaluate the model in a zero-shot setting and use the robot-centric map as a tool for local navigation. Additionally, we provide the ground-truth object locations to analyze the VLM’s decision-making performance under ideal conditions. Few-shot experiments, the impact of noisy maps and the use of images with polar actions as alternative for local navigation, are evaluated separately in Section IV-D.

Stopping condition. Unlike prior work that uses a dedicated VLM for success evaluation, in our setup human experts supervise all tasks and manually stop execution when the task is successfully completed, unless the VLM explicitly reports completion. Because the VLM can get stuck in infinite loops during execution, we define an early-stopping condition that instructs the VLM to skip the current subgoal and continue to the next one. Specifically, if the VLM fails to accomplish a subgoal after nine tool calls since the previous subgoal (a threshold derived from human performance statistics), we inform the VLM to abort that subgoal.

D. Ablation Studies

We evaluate the performance of our method under noisy conditions, specifically using a semantic map that contains false positives introduced by the object detector. This scenario is particularly challenging for a VLM agent, which relies heavily on the estimated locations of objects. When the robot navigates toward a target object that is actually a false positive, the VLM must 1) verify whether the object is an actual false positive in the map, 2) perform local exploration to search for the correct object nearby, and 3) if unsuccessful, navigate to an alternative map location for the same object.

We conduct seven trials per task category using the noisy map produced by our mapping framework. For each task, we evaluate three agents: a human operator, a VLM-zero-shot agent, and a VLM-few-shot agent. In contrast to the zero-shot setting, the VLM-few-shot agent receives example reasoning demonstrations in addition to the context description. These demonstrations illustrate situations such as reaching an incorrect navigation target, failing to execute a tool, or detecting a plant in front of the robot but outside the manipulator’s reachable workspace. To reduce token usage, the demonstrations include only natural-language scene descriptions and reasoning steps, without images. The full demonstrations are provided in the supplementary material.

We also consider two modes for local navigation: one using a robot-centric map, and another using the front camera augmented with potential actions. Both modes provide guidance for forward motion and in-place rotations, as described in Section III-A. For these ablations, we use the most complex polyculture environment, which includes more crop types and therefore produces noisier detections. A single precomputed noisy map is used for all runs to ensure fair comparison.

As in earlier experiments, we stop the agent once the task is successfully completed. Additionally, if the agent fails

to reach a navigation target after nine tool calls, we halt execution and instruct the agent to skip that target.

V. RESULTS AND DISCUSSION

A. Main Results

Result 1: Human operators consistently outperform zero-shot VLM control across all metrics Human operators demonstrate consistently superior performance across all task categories and environments. Averaged over the full task set, human success rates are high for both simple and complex scenarios, including multi-target and multi-plant conditions (Last row of Table I). In contrast, zero-shot VLM control exhibits substantial degradation as task complexity increases. While VLM performance is adequate for simpler tasks, success rates drop to 42.11% in multi-plant single-target problems and to 9.38% in multi-plant multi-target scenarios (Rows 3 and 4 of Table I).

This gap is preserved even in visually complex environments. In the complex polyculture environment, humans maintain 100% success across all categories (Table II), whereas VLM success ranges from 80.95-100% (Rows 1 and 2 of Table II) in single-plant tasks down to 27.27–31.58% in multi-plant tasks (Rows 3 and 4 of Table II). SPL values follow the same trend, with humans consistently producing more direct and efficient trajectories. These findings highlight the robustness and adaptability of human operation compared to the brittleness of zero-shot VLM control under increasing environmental and task complexity.

Neither the human nor the VLM achieves 100% success in the simple polyculture or the monoculture. This is due to the experimental design defining a failure when the task required finding a specific color tomato on a selected plant. If the target was a green or yellow tomato, and the plant selected only had ripe red tomatoes, then this manipulation task was considered a failure. This choice was deliberate implemented to simplify the computation of metrics and avoid the replanning required in scenarios where the target was not present. Although this choice resulted in recorded “failures” that were artifacts of the task definition rather than actual performance errors, it was maintained to ensure a streamlined and consistent evaluation framework. Notably, this specific failure scenario did not occur during the human experiments in the complex polyculture environment, which consequently achieved a 100% success rate under the defined task parameters.

Result 2: VLM control performs reliably on simple single-plant, single-target tasks

Despite its limitations, the zero-shot VLM controller performs reliably on the simplest task category involving a single plant and a single target. Across all environments, the VLM achieves 86.7% average success—approaching the 92% achieved by human operators (Row 1 of Table I). In the complex polyculture environment, the VLM even reaches 100% success on this task, matching human performance.

These tasks represent minimal-horizon navigation problems where the target is visually salient and the required

TABLE I
MAIN RESULTS

Task Category	Operator	Number of Trials	Success Rate (%) ↑	Number of Tool Calls ↓	Task Completion Rate (%) ↑	SPL ↑
Single Plant - Single Target	Human	62	91.94	9.53±3.15	96.27±15.36	90.32
	Zero-Shot VLM	60	86.67	11.33±3.04	96.72±11.24	60.84
Single Plant - Multiple Target	Human	60	91.67	14.04±5.02	97.67±8.44	91.67
	Zero-Shot VLM	57	68.42	18.38±5.28	88.33±20.97	47.64
Multiple Plant - Single Target	Human	43	93.02	22.95±2.58	98.58±5.73	93.02
	Zero-Shot VLM	38	42.11	33.44±7.79	85.05±15.12	28.63
Multiple Plant - Multiple Target	Human	33	84.85	33.11±6.78	90.06±17.16	84.85
	Zero-Shot VLM	32	9.38	43.33±9.29	76.19±17.04	5.87
Average Over All Categories		198	90.37	19.91±4.38	97.14±11.67	89.97
		187	51.64	26.62±6.35	86.57±16.09	35.74

TABLE II
MAIN RESULTS COMPLEX POLYCULTURE ENVIRONMENT

Task Category	Operator	Number of Trials	Success Rate (%) ↑	Number of Tool Calls ↓	Task Completion Rate (%) ↑	SPL ↑
Single Plant - Single Target	Human	21	100.0	8.14±1.21	100.0±0.0	100.0
	Zero-Shot VLM	21	100.0	10.24±2.72	100.0±0.0	68.44
Single Plant - Multiple Target	Human	21	100.0	11.81±2.52	100.0±0.0	100.0
	Zero-Shot VLM	21	80.95	16.94±3.04	92.86±15.70	52.97
Multiple Plant - Single Target	Human	19	100.0	22.74±1.37	100.0±0.0	100.0
	Zero-Shot VLM	19	31.58	38.33±10.81	81.58±15.08	24.65
Multiple Plant - Multiple Target	Human	11	100.0	32.45±6.53	100.0±0.0	100.0
	Zero-Shot VLM	11	27.27	43.33±9.29	83.55±15.81	17.07

TABLE III
MAIN RESULTS SIMPLE POLYCULTURE ENVIRONMENT

Task Category	Operator	Number of Trials	Success Rate (%) ↑	Number of Tool Calls ↓	Task Completion Rate (%) ↑	SPL ↑
Single Plant - Single Target	Human	21	85.71	12.28±4.08	93.76±21.47	80.95
	Zero-Shot VLM	19	73.68	14.07±2.25	97.53±5.67	57.44
Single Plant - Multiple Target	Human	19	94.74	18.00±5.13	99.21±3.35	94.74
	Zero-Shot VLM	17	70.59	20.08±8.28	88.82±25.81	55.54
Multiple Plant - Single Target	Human	14	92.86	24.00±3.74	99.21±2.83	92.86
	Zero-Shot VLM	9	33.33	29.67±1.89	81.44±16.49	26.18
Multiple Plant - Multiple Target	Human	13	84.62	29.64±5.07	91.85±26.56	84.62
	Zero-Shot VLM	11	0.00	NA	66.73±16.33	0.00

TABLE IV
MAIN RESULTS MONOCULTURE ENVIRONMENT

Task Category	Operator	Number of Trials	Success Rate (%) ↑	Number of Tool Calls ↓	Task Completion Rate (%) ↑	SPL ↑
Single Plant - Single Target	Human	20	90.00	8.39±1.42	95.00±15.00	90.00
	Zero-Shot VLM	20	85.00	10.41±2.52	92.50±17.85	56.08
Single Plant - Multiple Target	Human	20	80.00	12.50±4.69	93.75±13.40	80.00
	Zero-Shot VLM	19	52.63	18.80±1.94	82.89±19.95	34.68
Multiple Plant - Single Target	Human	10	80.00	21.75±1.64	95.00±10.62	80.00
	Zero-Shot VLM	10	70.00	30.86±1.96	94.90±7.79	38.39
Multiple Plant - Multiple Target	Human	9	66.67	40.67±3.09	97.33±3.77	66.67
	Zero-Shot VLM	10	0.00	NA	78.50±14.07	0.00

action sequence is short (see a sample episode in Fig. 1). Under these conditions, the VLM generates coherent and stable plans, reflected in consistent task completion rates and modest tool call counts relative to more complex scenarios. This result demonstrates that zero-shot vision-language-grounded control is viable for simple, well-structured agricultural tasks.

Result 3: VLMs are less efficient than Human Operators

Across all task categories, VLM control is less efficient than human teleoperation, as reflected in tool call counts and SPL metrics. Human operators typically complete tasks using about 9–11 tool calls for simple cases and 23–33 calls for multi-plant problems. The VLM consistently exceeds these values, requiring 11–18 calls for simple tasks and 33–43 calls in complex settings.

Higher tool call counts indicate more frequent replanning, corrective actions, and uncertain decision-making. Correspondingly, the VLM’s SPL scores remain well below those of humans, even in successful trials. This pattern suggests that while the VLM can infer reasonable high-level strategies, it lacks the precision and spatial efficiency of human operators, leading to longer and more circuitous behaviors. These behavioral inefficiencies present an important limitation for real-time robotic deployment.

Result 4: Environmental Complexity Degrades VLM Performance

Environmental complexity has a pronounced and disproportionate effect on VLM performance. In the most challenging environment—characterized by dense foliage, occlusion, irregular geometry, and visual noise—human performance remains perfect (100% across all categories). Zero-shot VLM control, however, degrades substantially. Success rates fall to 80.95% in single-plant multi-target tasks (Row 2 in Table II) and to 27.27% and 31.58% in multi-plant conditions (Rows 3 and 4 Table II). SPL similarly decreases, and tool call counts increase significantly, indicating repeated attempts to re-establish grounding and recover from planning failures.

These results illustrate that complex visual structure and longer horizon tasks impose a strong burden on the VLM’s spatial reasoning and perception-action grounding. Unlike human operators, who leverage contextual understanding and adaptive heuristics, the VLM struggles to maintain consistent target tracking and to plan long-horizon sequences in cluttered environments. Thus, scene complexity is a large factor contributing to failure for zero-shot VLM-based control.

B. Ablation Results

Tables V and VI present the results obtained with noisy semantic maps. Compared to Table I, which uses ground-truth maps, the zero-shot VLM agent experiences a drop of approximately 12% in success rate and 37% in completion rate due to map noise. These results highlight the challenges of uncertainty in complex environments and the need for more robust and adaptive decision-making strategies.

The results in Tables V and VI do not indicate a clear advantage for the VLM-few-shot agent over its zero-shot

counterpart. In some task categories, the few-shot agent even exhibits lower success and completion rates. On average across categories, the zero-shot VLM achieves a 7% higher success rate than the few-shot agent. One possible reason is the lack of visual examples in the demonstrations: providing only language descriptions without images may hinder proper grounding. We also observed during execution that the VLM agent’s performance degrades as the context window grows over time. This behavior, attributable to limitations of transformer attention mechanisms, has been reported in prior studies and remains an active research topic [46].

Furthermore, across multiple task categories, the agent using the front camera with overlaid polar actions (Table V) achieves, on average, a 7% higher success and completion rate than the agent using a robot-centric map (Table VI). This may be because VLMs are not necessarily trained with top-down semantic occupancy maps, making image-space planning more intuitive for them. Fine-tuning VLMs with 2D semantic occupancy maps may be necessary to fully leverage their spatial and semantic information.

C. Failure Cases

Failure Mode 1: Target Identification Errors

The VLM frequently demonstrated errors in basic object categorization, leading to downstream failures in navigation and manipulation. These errors included confusing visually similar produce—such as interpreting yellow tomatoes as ripe or green tomatoes—and misidentifying red bell peppers or tomatoes as strawberries. In some cases, the model incorrectly distinguished between plant species altogether. These failures indicate that, despite access to high-resolution imagery and semantic map metadata, the model may rely on unstable visual heuristics or incomplete contextual reasoning. Such misclassifications often propagated through the control loop, producing incorrect subgoal selection or premature task termination.

Beyond broad object class errors, the VLM struggled to correctly interpret fine-grained attributes such as color, plant part, or ripeness level. Sometimes, red tomatoes were “labeled ‘less ripe’” or selected the wrong instance within a cluster when multiple visually similar options were present. Attribute-specific errors were especially common for tasks requiring differentiation among leaves, stems, and fruit, where the model occasionally centered on or captured images of the wrong part despite the correct object being in view. These issues suggest that attribute-based recognition remains a weak point, even when class-level recognition appears correct.

Failure Mode 2: Redundant or Repetitive Behavior

A recurring behavioral pattern involved the model repeatedly centering the same target without making forward progress toward approaching or capturing it. In several instances, the VLM entered loops where it continually issued centering commands, apparently satisfied with the visual framing yet failing to advance to the next step of the task. This also occurred during image capture, where the model would

TABLE V
ABLATION STUDY RESULTS (COMPLEX POLYCULTURE ENVIRONMENT, NOISY MAP, POLAR ACTIONS)

Task Category	Operator	Number of Trials	Success Rate (%) ↑	Number of Tool Calls ↓	Task Completion Rate (%) ↑	SPL ↑
Single Plant - Single Target	Human	7	100.00	12.43±4.72	100.00±0.00	100.00
	Zero-Shot VLM	7	85.71	10.17±1.46	85.71±34.99	83.90
	Few-Shot VLM	7	85.71	10.17±1.34	85.71±34.99	79.30
Single Plant - Multiple Target	Human	7	100.00	15.86±2.75	100.00±0.00	100.00
	Zero-Shot VLM	7	28.57	21.50±3.50	53.57±38.80	28.57
	Few-Shot VLM	7	42.86	19.00±2.45	75.00±32.73	42.37
Multiple Plant - Single Target	Human	7	100.00	28.14±1.73	100.00±0.00	100.00
	Zero-Shot VLM	7	42.86	31.00±5.66	81.00±18.67	32.91
	Few-Shot VLM	7	14.29	31.00±0.00	52.43±30.25	13.49
Multiple Plant - Multiple Target	Human	7	100.00	35.43±5.39	100.00±0.00	100.00
	Zero-Shot VLM	7	28.57	37.50±8.50	52.00±34.12	18.74
	Few-Shot VLM	7	0.00	NA	45.86±29.78	0.00
Average Over All Categories	Human	28	100.00	22.96±3.65	100.00±0.00	100.00
	Zero-Shot VLM	28	46.43	25.04±4.78	68.07±31.64	41.03
	Few-Shot VLM	28	35.72	20.06±1.26	64.75±31.94	33.79

TABLE VI
ABLATION STUDY RESULTS (COMPLEX POLYCULTURE ENVIRONMENT, NOISY MAP, ROBOT-CENTRIC MAP)

Task Category	Operator	Number of Trials	Success Rate (%) ↑	Number of Tool Calls ↓	Task Completion Rate (%) ↑	SPL ↑
Single Plant - Single Target	Human	7	100.00	11.29±2.25	100.00±0.00	100.00
	Zero-Shot VLM	7	57.14	11.75±2.86	64.29±44.03	44.07
	Few-Shot VLM	7	71.43	9.80±0.98	78.57±36.42	55.71
Single Plant - Multiple Target	Human	7	100.00	16.43±1.40	100.00±0.00	100.00
	Zero-Shot VLM	7	42.86	19.00±2.16	50.00±46.29	29.88
	Few-Shot VLM	7	57.14	16.75±0.83	67.86±43.74	48.68
Multiple Plant - Single Target	Human	7	100.00	30.29±4.16	100.00±0.00	100.00
	Zero-Shot VLM	7	14.29	38.00±0.00	49.86±28.14	11.28
	Few-Shot VLM	7	0.00	NA	57.29±25.00	0.00
Multiple Plant - Multiple Target	Human	7	100.00	34.29±6.09	100.00±0.00	100.00
	Zero-Shot VLM	7	42.86	44.00±14.45	76.29±23.36	35.87
	Few-Shot VLM	7	0.00	NA	49.57±19.27	0.00
Average Over All Categories	Human	28	100.00	23.08±3.48	100.00±0.00	100.00
	Zero-Shot VLM	28	39.29	28.19±4.87	60.11±35.46	30.28
	Few-Shot VLM	28	32.14	13.28±0.90	63.32±31.11	26.10

repeatedly reframe a target it had already documented, or unnecessarily reacquire the same viewpoint from nearly identical camera poses. Such patterns indicate a disconnect between visual satisfaction criteria and the task-level state machine designed to govern completion.

The model also exhibited repetitive navigation behavior, reselecting the same plant or the same goal location after completion. In some episodes, it captured the same image twice due to relying solely on the most recent camera frame, effectively forgetting previously accomplished subtasks. In others, it navigated back to a plant it had already visited, or misinterpreted a previously achieved goal as the next required target. These loops reflect inconsistencies in temporal reasoning and insufficient handling of task memory within the prompt or system context.

Failure Mode 3: Incorrect Self-Evaluation Several failures stemmed from the model’s inability to correctly evaluate the results of its own actions. In several episodes, the VLM believed it had successfully completed a subgoal even when the captured image did not contain the required element. Conversely, it sometimes assumed it had failed despite having

captured the correct target, prompting further unnecessary exploration or repeated re-execution of a completed step. These errors occasionally triggered cascades of redundant behavior, such as revisiting plants or recentering previously captured objects. Even when user feedback was provided, the model would sometimes integrate it incorrectly or continue to question its progress. These findings highlight fundamental challenges in perception-action grounding, particularly in interpreting visual feedback in the context of multi-stage tasks.

Failure Mode 4: Misuse or Ignoring Human Feedback

Although the system is designed to leverage human input for correction and confirmation, the VLM often misused or misinterpreted this feedback channel. At times, the model ignored user prompts to proceed to the next subgoal, continuing to refine an already complete image. In other cases, it requested confirmation at inappropriate times—such as immediately after completing a subgoal or before attempting the next action—leading to unnecessary slowdowns. The model occasionally asked for guidance despite having sufficient information to continue independently, or applied user feedback

in an overly literal or incorrect manner. These behaviors illustrate a lack of reliable grounding for human-provided signals, and highlight broader challenges in building VLM-driven systems that must balance autonomy with interactive correction.

Failure Mode 5: Miscellaneous Behaviors A variety of additional behaviors fell outside the primary failure categories but remain informative for understanding the system’s overall robustness. These include over-collecting images due to ambiguous task interpretation, completing goals out of order, or extracting an incorrect number of subgoals from natural-language instructions. The model sometimes relied on stale or noisy global map information instead of using available local camera feedback, or hallucinated plant locations entirely. Navigation failures were also common, such as getting stuck, approaching the wrong plant, moving backward unnecessarily, or attempting to explore nonexistent vegetation. The VLM occasionally neglected to use the robot-centric map for local navigation or misused polar actions when available. Despite these failures, some episodes showcased unexpectedly competent behaviors, such as clever backward camera use or successful fallback to the local map after a global navigation failure. These mixed outcomes underscore both the promise and instability of current VLM control in structured agricultural environments.

VI. LIMITATIONS

The VLM agent performs well on short-horizon tasks under noiseless conditions. While the VLM agent achieves performance close to that of humans on short-horizon tasks, its performance deteriorates on long-horizon tasks. Long-horizon tasks require a long context window, which remains an active research challenge for both LLMs and VLMs. This limitation is also evident when providing demonstrations to the VLM agent: the model often fails to capture fine-grained details or desired behaviors provided in the demonstrations. Overall, our experiments showed that a longer context window leads to a performance drop compared to the zero-shot agent. The performance degradation is exacerbated when using noisy maps. In many cases, the VLM does not even detect false-positive objects in the map. These misdetections may be attributed to the overconfidence commonly exhibited by VLMs, as reported in prior work [47]. However, they may also stem from dataset bias, since the model is evaluated in a simulated environment whose visual appearance differs significantly from the real images used during training.

The VLM agent lacks robust spatial reasoning. Crop-monitoring tasks require the ability to reason about proximity to objects, object size, occlusions, and the spatial relationships between objects and the robot. While humans excel at these skills, the VLM agent shows substantial deficiencies, leading to failures and inefficient task execution. A key reason for this limitation is that most VLMs are trained primarily on image–text pairs, where spatial relationships are rarely annotated explicitly. As a result, the model learns strong associations between objects and their semantic la-

bels but develops only weak representations of geometric structure, distance, and 3D layout. Furthermore, because VLMs operate on static 2D images, they lack an explicit notion of depth or egocentric spatial context. Fine-tuning the model on spatial-reasoning tasks may help improve the VLM agent’s performance in crop monitoring. Additionally, incorporating heterogeneous data modalities such as videos or 3D representations may be necessary to fully unlock the spatial reasoning capabilities of these agents.

The reliance on large-scale foundation models introduces significant latency, limiting the system’s applicability in time-critical robotic operations. The high inference cost necessitates the use of sparse image observations rather than continuous visual streams, which forces the agent to make decisions based on snapshot data that may miss dynamic environmental cues. A lightweight VLM would not only reduce inference time, enabling smoother real-time control, but could also support high-frequency video input. Processing video rather than static frames would provide the model with richer temporal and 3D cues, potentially resolving the spatial ambiguity and context grounding issues observed in our experiments.

VII. CONCLUSION AND FUTURE WORK

In this work, we introduced a novel, modular framework for visual-language-guided task planning in horticultural environments. By interleaving input-source queries with a library of action primitives, our system enables mobile manipulators to perform flexible crop monitoring tasks using natural language instructions. We integrated open-vocabulary semantic occupancy maps and enriched camera observations to ground high-level reasoning in the physical environment. Our extensive evaluation in simulated monoculture and polyculture environments reveals a distinct dichotomy in current VLM capabilities for agricultural robotics. We found that zero-shot VLM agents perform robustly on short-horizon, single-target tasks, achieving success rates comparable to human operators. However, performance degrades significantly as task complexity increases. In long-horizon scenarios involving multiple plants and targets, the VLM struggled with spatial reasoning, efficient navigation, and context management, often resulting in redundant behaviors and lower success rates compared to expert run trials. Furthermore, our ablation studies demonstrated that system reliability is heavily dependent on map accuracy, with performance dropping notably when facing perception noise.

To bridge the gap between current capabilities and field-ready deployment, our future work will focus on addressing these spatial and temporal limitations. We aim to fine-tune small VLMs on agricultural datasets enriched with explicit spatial relationships and map data to enhance geometric reasoning. Additionally, we plan to incorporate richer input modalities, such as video streams or 3D scene representations, to improve depth perception and temporal understanding. Finally, to mitigate the performance degradation observed in long-horizon tasks, we will explore advanced

memory management techniques to overcome context window constraints and prevent the repetitive behaviors observed in our experiments.

REFERENCES

- [1] S. Getahun, H. Kefale, and Y. Gelaye, "Application of precision agriculture technologies for sustainable crop production and environmental sustainability: A systematic review," *The Scientific World Journal*, vol. 2024, no. 1, p. 2126734, 2024.
- [2] M. Spagnuolo, G. Todde, M. Caria, N. Furnitto, G. Schillaci, and S. Failla, "Agricultural robotics: A technical review addressing challenges in sustainable crop production," *Robotics*, vol. 14, no. 2, p. 9, 2025.
- [3] J. Cuaran, K. S. Ahluwalia, K. Koe, N. K. Uppalapati, and G. Chowdhary, "Active semantic mapping with mobile manipulator in horticultural environments," in *2025 IEEE International Conference on Robotics and Automation (ICRA)*. IEEE, 2025, pp. 12 716–12 722.
- [4] Y. Pan, F. Magistri, T. Läbe, E. Marks, C. Smitt, C. McCool, J. Behley, and C. Stachniss, "Panoptic mapping with fruit completion and pose estimation for horticultural robots," in *2023 IEEE/RSJ International Conference on Intelligent Robots and Systems (IROS)*. IEEE, 2023, pp. 4226–4233.
- [5] H. Freeman and G. Kantor, "Autonomous apple fruitlet sizing with next best view planning," in *2024 IEEE International Conference on Robotics and Automation (ICRA)*. IEEE, 2024, pp. 15 847–15 853.
- [6] C. Lehnert, D. Tsai, A. Eriksson, and C. McCool, "3d move to see: Multi-perspective visual servoing towards the next best view within unstructured and occluded environments," in *2019 IEEE/RSJ International Conference on Intelligent Robots and Systems (IROS)*. IEEE, 2019, pp. 3890–3897.
- [7] T. Zaenker, C. Smitt, C. McCool, and M. Bennewitz, "Viewpoint planning for fruit size and position estimation," in *2021 IEEE/RSJ International Conference on Intelligent Robots and Systems (IROS)*. IEEE, 2021, pp. 3271–3277.
- [8] W. Huang, P. Abbeel, D. Pathak, and I. Mordatch, "Language models as zero-shot planners: Extracting actionable knowledge for embodied agents," in *International conference on machine learning*. PMLR, 2022, pp. 9118–9147.
- [9] M. Ahn, A. Brohan, N. Brown, Y. Chebotar, O. Cortes, B. David, C. Finn, C. Fu, K. Gopalakrishnan, K. Hausman *et al.*, "Do as i can, not as i say: Grounding language in robotic affordances," *arXiv preprint arXiv:2204.01691*, 2022.
- [10] W. Huang, F. Xia, T. Xiao, H. Chan, J. Liang, P. Florence, A. Zeng, J. Tompson, I. Mordatch, Y. Chebotar *et al.*, "Inner monologue: Embodied reasoning through planning with language models," *arXiv preprint arXiv:2207.05608*, 2022.
- [11] J. Liang, W. Huang, F. Xia, P. Xu, K. Hausman, B. Ichter, P. Florence, and A. Zeng, "Code as policies: Language model programs for embodied control," *arXiv preprint arXiv:2209.07753*, 2022.
- [12] D. Goetting, H. G. Singh, and A. Loquercio, "End-to-end navigation with vlms: Transforming spatial reasoning into question-answering," in *Workshop on Language and Robot Learning: Language as an Interface*, 2024.
- [13] S. Nasiriany, F. Xia, W. Yu, T. Xiao, J. Liang, I. Dasgupta, A. Xie, D. Driess, A. Wahid, Z. Xu *et al.*, "Pivot: Iterative visual prompting elicits actionable knowledge for vlms," *arXiv preprint arXiv:2402.07872*, 2024.
- [14] P. Wu, Y. Mu, B. Wu, Y. Hou, J. Ma, S. Zhang, and C. Liu, "Voronav: Voronoi-based zero-shot object navigation with large language model," *arXiv preprint arXiv:2401.02695*, 2024.
- [15] P. Zhi, Z. Zhang, Y. Zhao, M. Han, Z. Zhang, Z. Li, Z. Jiao, B. Jia, and S. Huang, "Closed-loop open-vocabulary mobile manipulation with gpt-4v," *arXiv preprint arXiv:2404.10220*, 2024.
- [16] H. Jiang, B. Huang, R. Wu, Z. Li, S. Garg, H. Nayyeri, S. Wang, and Y. Li, "Roboexp: Action-conditioned scene graph via interactive exploration for robotic manipulation," *arXiv preprint arXiv:2402.15487*, 2024.
- [17] M. Elnoor, K. Weerakoon, G. Seneviratne, R. Xian, T. Guan, M. K. M. Jaffar, V. Rajagopal, and D. Manocha, "Robot navigation using physically grounded vision-language models in outdoor environments," *arXiv preprint arXiv:2409.20445*, 2024.
- [18] C. Huang, O. Mees, A. Zeng, and W. Burgard, "Visual language maps for robot navigation," *arXiv preprint arXiv:2210.05714*, 2022.
- [19] D. Shah, B. Osiński, S. Levine *et al.*, "Lm-nav: Robotic navigation with large pre-trained models of language, vision, and action," in *Conference on robot learning*. PMLR, 2023, pp. 492–504.
- [20] A. Werby, C. Huang, M. Büchner, A. Valada, and W. Burgard, "Hierarchical open-vocabulary 3d scene graphs for language-grounded robot navigation," in *First Workshop on Vision-Language Models for Navigation and Manipulation at ICRA 2024*, 2024.
- [21] J. Chen, B. Lin, R. Xu, Z. Chai, X. Liang, and K.-Y. K. Wong, "Mapgpt: Map-guided prompting with adaptive path planning for vision-and-language navigation," *arXiv preprint arXiv:2401.07314*, 2024.
- [22] L. Zhong, C. Gao, Z. Ding, Y. Liao, H. Ma, S. Zhang, X. Zhou, and S. Liu, "Topv-nav: Unlocking the top-view spatial reasoning potential of mllm for zero-shot object navigation," *arXiv preprint arXiv:2411.16425*, 2024.
- [23] M. Haghhighat, A. Saleh, and M. R. Azghadi, "Multimodal language models in agriculture: A tutorial and survey," *Authorea Preprints*, 2025.
- [24] M. A. Zuzuáregui and S. Carpin, "Leveraging llms for mission planning in precision agriculture," *arXiv preprint arXiv:2506.10093*, 2025.
- [25] R. E. Fikes and N. J. Nilsson, "Strips: A new approach to the application of theorem proving to problem solving," *Artificial intelligence*, vol. 2, no. 3-4, pp. 189–208, 1971.
- [26] L. P. Kaelbling and T. Lozano-Pérez, "Hierarchical task and motion planning in the now," in *2011 IEEE international conference on robotics and automation*. IEEE, 2011, pp. 1470–1477.
- [27] J. Wolfe, B. Marthi, and S. Russell, "Combined task and motion planning for mobile manipulation," in *Proceedings of the International Conference on Automated Planning and Scheduling*, vol. 20, 2010, pp. 254–257.
- [28] K. Zhang, E. Lucet, J. A. D. Sandretto, S. Kchir, and D. Filliat, "Task and motion planning methods: applications and limitations," in *ICINCO 2022-19th International Conference on Informatics in Control, Automation and Robotics*. SCITEPRESS-Science and Technology Publications, 2022, pp. 476–483.
- [29] S. S. Raman, V. Cohen, I. Idrees, E. Rosen, R. Mooney, S. Tellex, and D. Paulius, "Cape: Corrective actions from precondition errors using large language models," in *2024 IEEE International Conference on Robotics and Automation (ICRA)*. IEEE, 2024, pp. 14 070–14 077.
- [30] J. Styrud, M. Iovino, M. Norrlöf, M. Björkman, and C. Smith, "Automatic behavior tree expansion with llms for robotic manipulation," *arXiv preprint arXiv:2409.13356*, 2024.
- [31] A. Majumdar, A. Ajay, X. Zhang, P. Putta, S. Yenamandra, M. Henaff, S. Silwal, P. Mcvay, O. Maksymets, S. Arnaud *et al.*, "Openeqa: Embodied question answering in the era of foundation models," in *Proceedings of the IEEE/CVF conference on computer vision and pattern recognition*, 2024, pp. 16 488–16 498.
- [32] M. F. Ginting, D.-K. Kim, X. Meng, A. Reinke, B. J. Krishna, N. Kayhani, O. Peltzer, D. D. Fan, A. Shaban, S.-K. Kim *et al.*, "Enter the mind palace: Reasoning and planning for long-term active embodied question answering," *arXiv preprint arXiv:2507.12846*, 2025.
- [33] G. Lan, K. Qu, R. Zurbrügg, C. Chen, C. E. Mower, H. Bou-Ammar, and M. Hutter, "Experience is the best teacher: Grounding vlms for robotics through self-generated memory," *arXiv preprint arXiv:2507.16713*, 2025.
- [34] Y. Hu, F. Lin, T. Zhang, L. Yi, and Y. Gao, "Look before you leap: Unveiling the power of gpt-4v in robotic vision-language planning," *arXiv preprint arXiv:2311.17842*, 2023.
- [35] U. Nawaz, M. Awais, H. Gani, M. Naseer, F. Khan, S. Khan, and R. M. Anwer, "Agriclip: Adapting clip for agriculture and livestock via domain-specialized cross-model alignment," *arXiv preprint arXiv:2410.01407*, 2024.
- [36] M. Awais, A. H. S. A. Alharthi, A. Kumar, H. Cholakkal, and R. M. Anwer, "Agrogpt: Efficient agricultural vision-language model with expert tuning," in *2025 IEEE/CVF Winter Conference on Applications of Computer Vision (WACV)*. IEEE, 2025, pp. 5687–5696.
- [37] K. Zhang, L. Ma, B. Cui, X. Li, B. Zhang, and N. Xie, "Visual large language model for wheat disease diagnosis in the wild," *Computers and Electronics in Agriculture*, vol. 227, p. 109587, 2024.
- [38] K. N. Quoc, L. L. T. Thu, and L.-D. Quach, "A vision-language

foundation model for leaf disease identification,” *arXiv preprint arXiv:2505.07019*, 2025.

- [39] Y. Zhou, H. Yan, K. Ding, T. Cai, and Y. Zhang, “Few-shot image classification of crop diseases based on vision–language models,” *Sensors*, vol. 24, no. 18, p. 6109, 2024.
- [40] R. Shinoda, N. Inoue, H. Kataoka, M. Onishi, and Y. Ushiku, “Agrobench: Vision-language model benchmark in agriculture,” *arXiv preprint arXiv:2507.20519*, 2025.
- [41] P. Yu and B. Lin, “A framework for agricultural intelligent analysis based on a visual language large model,” *Applied Sciences*, vol. 14, no. 18, p. 8350, 2024.
- [42] A. Hornung, K. M. Wurm, M. Bennewitz, C. Stachniss, and W. Burgard, “Octomap: An efficient probabilistic 3d mapping framework based on octrees,” *Autonomous robots*, vol. 34, pp. 189–206, 2013.
- [43] C. Kaiser and M. Ernst, “High tunnel tomatoes,” *University of Kentucky College of Agriculture, Food and Environment Cooperative Extension Service, Lexington*, 2012.
- [44] D. Waterer, “Yields and economics of high tunnels for production of warm-season vegetable crops,” *HortTechnology*, vol. 13, no. 2, pp. 339–343, 2003.
- [45] D. Batra, A. Gokaslan, A. Kembhavi, O. Maksymets, R. Mottaghi, M. Savva, A. Toshev, and E. Wijmans, “Objectnav revisited: On evaluation of embodied agents navigating to objects,” *arXiv preprint arXiv:2006.13171*, 2020.
- [46] S. Chen, Z. Lin, Y. Polyanskiy, and P. Rigollet, “Critical attention scaling in long-context transformers,” *arXiv preprint arXiv:2510.05554*, 2025.
- [47] T. Groot and M. Valdenegro-Toro, “Overconfidence is key: Verbalized uncertainty evaluation in large language and vision-language models,” *arXiv preprint arXiv:2405.02917*, 2024.